

Analysis of the confinement of RC hollow columns wrapped with FRP

G.P. Lignola, A. Prota, G. Manfredi & E. Cosenza

Department of Structural Engineering DIST, University of Naples Federico II, Naples, Italy

ABSTRACT: This paper presents a theoretical model for the analysis of fiber-reinforced polymer (FRP) confined hollow reinforced concrete (RC) sections as found in many tall bridge piers. FRP confinement systems effectiveness have been studied focusing on solid columns while very little has been done about hollow sections. In order to study the behavior of square hollow sections subjected to combined axial load and bending, a total of 7 specimens have been tested, representing, in a scale 1:5, typical square hollow bridge piers. The strengthening scheme consisted of unidirectional Carbon FRP laminates applied in the transverse direction. The proposed model is able to estimate confinement effectiveness in the case of hollow sections. Relevant parameter was the relative wall thickness. Theoretical results, in excellent agreement with authors' sets of experimental data, show that FRP jacketing can enhance the ultimate load and the ductility also in the case of hollow concrete cross sections.

1 INTRODUCTION

1.1 *Hollow cross section confinement*

Compression column elements potentially support a variety of structures such as bridge decks and floor slabs. Columns vary in physical shape depending on their application, although typically they are either circular or rectangular, solid or hollow, for the simplicity of construction.

Various spectacular concrete bridges including hollow piers have been constructed throughout the world particularly in Europe, United States and Japan, where high seismic actions and natural boundaries require high elevation infrastructures. Hollow concrete cross sections are usually found in tall bridge piers. High elevation bridges with very large size columns are constructed to resist high moment and shear demands. In particular, bridge piers designed in accordance with old design codes may suffer severe damage during seismic events, caused by insufficient shear or flexural strength, low ductility and inadequate reinforcement detailing. Many parameters may influence the overall hollow column response such as: the shape of the section, the amount of the longitudinal and transverse reinforcement, the cross section thickness, the axial load ratio and finally the material strength of concrete (core and cover) and steel (reinforcement).

Apart from the possible human victims, severe earthquake damage on bridges results in economic losses in the form of significant repair or replace-

ment costs and disruption of traffic and transportation. For these reasons, important bridges are required to suffer only minor, repairable damage and maintain immediate occupancy after an earthquake to facilitate relief and rescue operations. Most of the existing bridges worldwide were designed before their seismic response had been fully understood and modern codes had been introduced; consequently they represent a source of risk in earthquake-prone regions.

Recent earthquakes in urban areas have repeatedly demonstrated the vulnerability of older structures to seismic actions, also those made by reinforced concrete, with deficient shear strength, low flexural ductility, insufficient lap splice length of the longitudinal bars and, very often, inadequate seismic detailing, as well as, in many cases, insufficient flexural capacity.

The only available answer to the aforementioned problems were either to rebuild the structure or to use standard restoring techniques (i.e. section enlargement, steel jacketing and others) that would have had a high social and economical impact as well as structural consequences such as increase in self weight consequently with a negative contribution to foundations and to the seismic response of the overall structure.

FRP materials as an alternative approached the construction market as a viable, cost and time effective solution for upgrading and retrofitting existing concrete structures. FRP confinement systems effec-

tiveness have been extensively studied in the last years focusing on solid columns while very little research has been done about hollow cross sections.

1.2 Research impact and objectives

The objective of the proposed investigation is to evaluate the behavior of square hollow bridge cross sections retrofitted with FRP composites materials used as external jacketing. The influence of external loading conditions, namely pure compression and combined flexure and compression has been studied in order to determine the available ductility of unstrengthened and strengthened rectangular hollow cross sections. This evaluation consists in an experimental phase undertaken in conjunction with analytical studies to predict and to model the results of the former tests. The development of design construction specifications and a refined methodology to design and assess hollow cross section members behavior under combined axial load and bending is the final output of the program.

2 EXPERIMENTAL CAMPAIGN

2.1 Test matrix and test set-up

Full-scale testing of these structures is out of the question, both for logistic and cost reasons, and also because data are needed prior to the design of the structure. Engineers thus have to rely on scale-model tests to predict the behavior of the prototypes and consequently to know how to estimate ultimate strains and stresses in the structures from the results obtained in scaled-down specimens. The probability of finding a serious flaw in a structural member increases with its size and varies with the type of material.

The experimental program has been planned on hollow columns in reduced scale. The scale factor 1:5 has then been chosen and tested specimens, reproducing in scale typical bridge piers, had hollow section external dimensions of $360 \times 360 \text{ mm}^2$ and walls thickness of 60 mm. The internal reinforcement was given by 16- $\phi 10$ longitudinal bars with 25 mm concrete cover and $\phi 4$ stirrups at 80 mm on center (Fig. 1).

The selection of the scale factor has been driven by two considerations: the attempt to study specimens whose dimensions were sufficiently large to represent the behavior of real piers and the need to respect laboratory constraints.

The hollow portion of the column had a height of 1.30 m and was made by foam-polystyrene, while the overall height of the specimen is 3 m.

The test matrix was designed in order to assess the FRP wrapping effectiveness in correspondence of three P/M ratios, which are three different neutral axis positions.

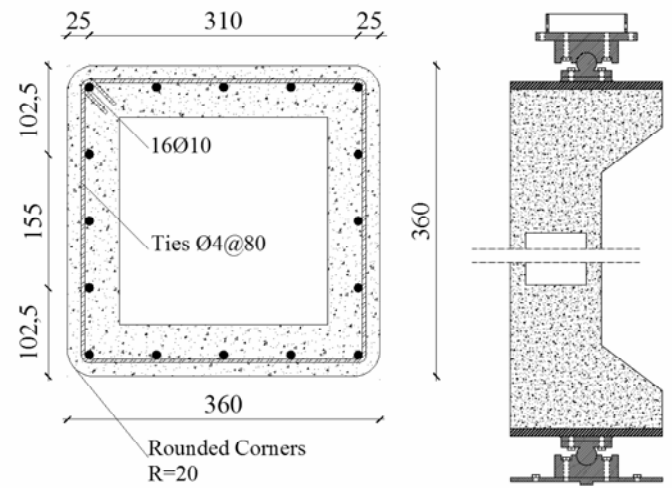


Figure 1. Specimen geometry.

Three eccentricities have been selected to study the behavior of the hollow members under P-M combinations carrying the neutral axis at ultimate load external to cross section ($e = 50 \text{ mm}$, fully compressed), at mid-height ($e = 200 \text{ mm}$), and close to compressed flange ($e = 300 \text{ mm}$). Accordingly three specimens are unstrengthened (Series U), while the second three are strengthened (Series S). A compressed unstrengthened specimen was also tested.

The matrix of tests done is reported in table 1, where e is the load eccentricity kept constant during each test. Note that a construction issue did not allow testing both specimens U1 and S1 with eccentricity of 50 mm; actual eccentricity was 52 mm and 80 mm.

In the U-series and S-series the two ends have been designed with corbels to allow the application of the axial load with the desired eccentricity as showed in figure 1, whereas the heads had solid sections in order to distribute the load and avoid local failures. In order to apply the axial load with the desired eccentricity, two open hinges have been designed (Fig. 1) to facilitate the centering of the specimen under the testing machine and to apply an eccentric axial load without shear and having free rotations at the two specimen ends.

Table 1. Test Matrix.

Specimen Code	Loading Condition	Eccentricity e (mm)
U0 - ...	Pure Compression	0
U1 - S1	Combined Compression and Flexure	52-80
U2 - S2		200
U3 - S3		300

2.2 Materials Characterization

Some tests have been executed on concrete and steel bars: during concrete pouring five specimens of plain concrete have been taken and nine pieces of

steel longitudinal bars ($\phi 10$) picked up. Concrete specimens have been crushed and test results show a mean compressive strength of 32 MPa.

Three series of steel bars have been also tested. The first one have been tested under tension, while the other two under compression with a Length to Diameter L/D ratio of 8 and 16 (to simulate the different free length of the compressed bar). Depending on the stirrup stiffness, the compressed longitudinal bar between two stirrups has different free length: the distance of the two testing grips have to be one or two times the stirrup spacing to simulate stirrups that are relative stiff or weak, respectively. A completely different behavior can be observed (Fig. 2) in the three cases: the instability in the compression case (buckling) corresponding to L/D=16 have been accounted for in the following analyses. Test results show a mean tensile strength of 600 MPa and a yield stress of 506 MPa (that in compression roughly correspond to buckling stress in the case of L/D = 16).

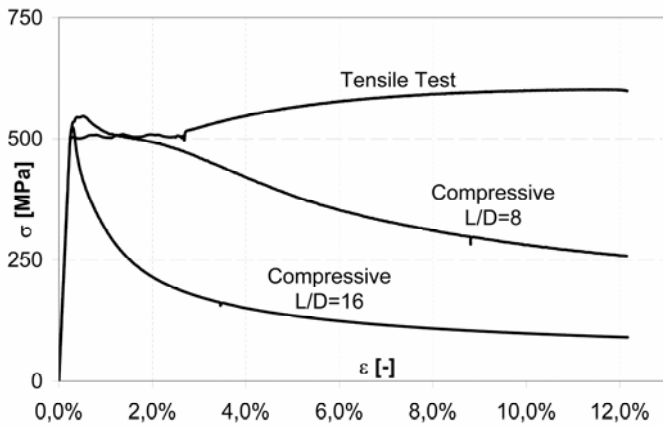


Figure 2. Steel bars characterization.

2.3 Strengthening scheme

Two plies of CFRP unidirectional fabric with density of 600 gr/m² have been applied in all S specimens for the entire specimen height (Fig. 3). Tensile modulus of elasticity of the CFRP material is 230 GPa and ultimate tensile strength is 3450 MPa. The fabrics have a nominal width of 400 mm and nominal thickness (dry) of 333 μ m.

The solid parts only have been further reinforced with a third layer of CFRP (Fig. 3) in order to avoid the occurrence of local failures in zones not of interest for the test but subjected to high stress concentrations.

The CFRP laminates were applied by manual lay-up in the transverse direction. Corners were rounded with a radius of 20 mm as prescribed in many codes and the two plies have been overlapped by 200 mm.

The number of installed plies was considered an upper limit that could be derived from an economical and technical analysis, also accounting for the scale reduction. On this scheme the CFRP rein-

forcement ratio is four times bigger than the stirrups reinforcement ratio. Nevertheless it has been observed that the influence of the number of layers of FRP on the solid section specimen under eccentric loading is not so pronounced as that of the specimen under concentric loading (Li & Hadi 2003).

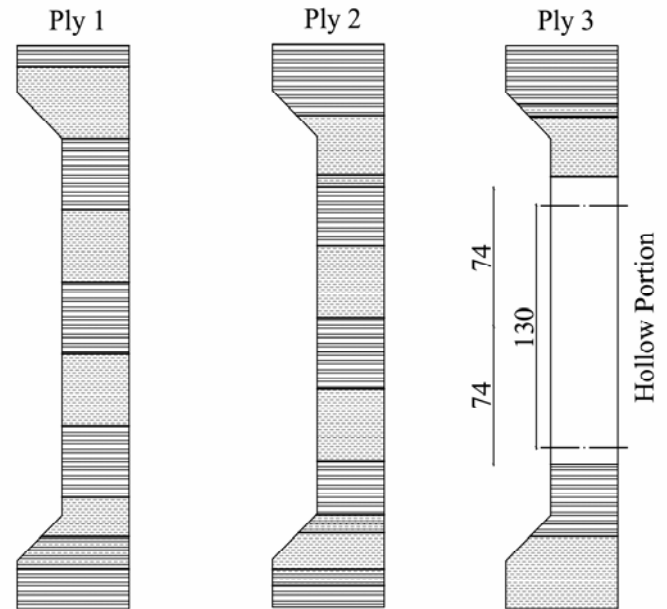


Figure 3. CFRP strengthening scheme.

The choice of carbon fibers over glass and aramid has been made since the former have not only better mechanical properties with respect to glass and aramid both in terms of ultimate strength and elastic modulus but also have the best durability performance in exposed environments, guaranteeing the longest life of the intervention.

Trade names of the FRP System materials adopted are reported in table 2.

Table 2. Adopted FRP system materials.

Material	Trade name
Fabric	MapeWrapC Uni-Ax 600/40
Primer	MapeWrap Primer1 A+B
Putty	MapeWrap12 A+B
Resin	MapeWrap31 A+B

2.4 Main experimental outcomes

Fundamental results and global outcomes of the experimental research in terms of strength and failure modes of the scaled hollow columns are given in (Lignola et al. 2007a,b). In the following, a brief summary will recall the main results in terms of strength, ductility and failure modes.

The failure of hollow members is strongly affected by the occurrence of premature mechanisms

(compressed bars buckling and unrestrained concrete cover spalling). FRP confinement does not change actual failure mode, but it is able to delay bars buckling and to let compressive concrete strains attain higher values, thus resulting in higher load carrying capacity of the column (strength improvement about 7% in the case of larger eccentricity and 19% in the case of smaller eccentricity) and significantly in ductility enhancement.

The ductility increments have been estimated through the comparison of curvature ductility μ_γ . In unstrengthened columns the curvature ductility ranged between 1 (brittle failure of U1 and U2) and 1.54 (specimen U3), while in the case of strengthened columns the curvature ductility increased significantly attaining values ranging between 3.07 and 8.27.

Actually the increment of ductility supplied by confinement corresponds also to a significant gain in terms of area under the curve that is proportional to the specific energy and can be also appreciated comparing the values of these specific energies and remarkable increases of dissipating capabilities for strengthened columns are found.

The maximum energy is recorded for the column S3. For instance the dissipated specific energy of S3 specimen is more than 7 times the dissipated specific energy of the brittle U3 specimen for the same eccentricity. Specific energy increment after peak at 80% of ultimate load is more than 3.71 times the specific energy at peak. This analysis evidenced a remarkable improvement of the seismic response of the wrapped columns: after peak load they kept a good load carrying capability, that is good energy dissipation.

The strength improvement was more relevant in the case of specimens loaded with smaller eccentricity, while the ductility improvement was more relevant in the case of bigger eccentricity. At lower levels of axial load also the brittle effect of reinforcement buckling was less noticeable.

3 THEORETICAL ANALYSIS

3.1 Section analysis: fiber model

Through the use of a fiber model that meshes the concrete cross-sectional geometry into a series of discrete elements/fibers, sections of completely arbitrary cross-sectional shape (including hollow prismatic cross sections) can be modeled. Tension stiffening effect, compressed bars buckling, concrete cover spalling and FRP confinement of concrete are included in the model (Lignola 2006).

The described numerical model uses nonlinear stress-strain relationships for concrete and steel. A reliable stress-strain behavior of concrete is necessary particularly when a member is subjected to

combined bending and axial load and confinement effects should be accounted for.

The stress-strain relationship of plain concrete under concentric loading is believed to be representative also of the behavior of concrete under eccentric loading.

3.2 Proposed hollow section confinement model

Two approaches were used to assess the behavior of the FRP confined hollow members. A first approach that considers the interaction of the four walls forming the hollow member has been proposed. This approach considers the interaction of the four walls forming the hollow member. The walls confinement have been analyzed according to the behavior observed in wall-like columns (Prota et al. 2006) similar to the behavior of the walls forming the hollow member. The transverse dilation of the compressed concrete walls stretches the confining device, which along with the other restrained walls applies an inward confining pressure. A detailed description of this approach can be found in (Lignola 2006).

A different approach, instead, that consider the confinement of the whole hollow section has been proposed (Lignola 2006). This confinement model for circular hollow sections has been extended to square hollow ones. The confining pressure is provided by an FRP jacket of the same thickness to an equivalent circular column of diameter D equal to the average side length. The model is able to estimate confinement effectiveness, which is different in the case of solid and hollow sections. The numerical predicted stress strain relationships for a solid section and for a hollow section with different R_i/R_o ratios, but constant relative confinement stiffness $E_t/(R_o-R_i)$ is depicted in figure 4.

A model based on the assumption that the increment of stress in the concrete is achieved without any out-of-plane strain was proposed (Braga et al. 2006). Plain strain conditions were adopted to simulate the confinement effect.

An elastic model (Fam & Rizkalla 2001) based on equilibrium and radial displacement compatibil-

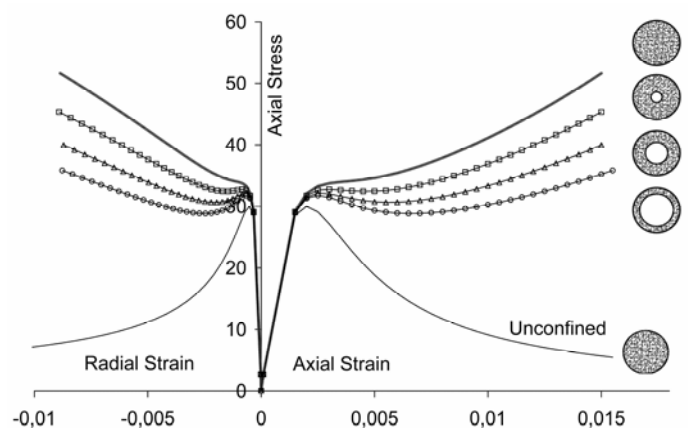


Figure 4. Proposed hollow section confinement model.

ity was presented adopting the equations proposed by *Mander et al. (1988)* through a step-by-step strain increment technique to trace the lateral dilation of concrete.

In the hypothesis of axial symmetry the radial displacement is the only displacement component and stress components (radial and circumferential) can be evaluated according to boundary conditions (i.e. applied external inward pressure and internal outward pressure). The dependence of the lateral strain with the axial strain is explicitly considered through radial equilibrium equations and displacement compatibility. Confining pressure q equation can be explicated in the form $q=q(\varepsilon_c)$, so that at each axial strain ε_c the confining pressure q exerted on concrete by the FRP jacket is associated:

$$q = \frac{v_c}{\frac{R_o}{E_f t} (1 - v_f) + \frac{1 + v_c}{E_c} \frac{R_o^2}{R_o^2 - R_i^2} \left[(1 - 2v_c) + \left(\frac{R_i}{R_o} \right)^2 \right]} \varepsilon_c \quad (1)$$

Previous equation (1) is based on linear elasticity theory for all the involved materials (E_c and v_c are concrete elastic modulus and Poisson's ratio respectively, while E_f and v_f are FRP elastic modulus and Poisson's ratio respectively), R_o and R_i are respectively the outer and inner radius of the hollow circular cross section, t is the thickness of the FRP wrap.

To account for the nonlinear behavior of concrete, a secant approach can be considered. The elastic modulus and the Poisson's ratio are function of the axial strain and of the confinement pressure q .

An iterative procedure is then performed to evaluate, at any given axial strain ε_c , the corresponding stress f_c , pertaining to a Mander's curve at a certain confining pressure $q(\varepsilon_c)$.

To simplify and to avoid an iterative procedure to determine the actual (step i) secant elastic modulus of concrete, this parameter is evaluated as the slope of the line connecting the origin and the previously evaluated (step $i-1$) stress-strain point.

The secant Poisson's ratio is used to obtain the lateral strain at a given axial strain in the incremental approach. The dilation of confined concrete is reduced by the confinement; therefore, the Poisson's ratio at a given axial strain level is lower in the presence of higher confining pressure. Fitting the results curve of many concrete cylinders tested under different confining hydrostatic pressures q with a second-order polynomial, a simplified linear relationships for ε_c under constant confining pressures is provided, and from regression analysis, it can be considered (*Fam & Rizkalla 2001*):

$$\frac{v_c}{v_{co}} = 1 + \frac{\varepsilon_c}{\varepsilon_{cc}} \left(0.719 + 1.914 \frac{q}{f'_{co}} \right) \quad (2)$$

where v_c is the actual Poisson's ratio at a given axial strain ε_c and actual confining pressure $q(\varepsilon_c)$. The ac-

tual peak confined concrete compressive strain (evaluated for the actual confining pressure q) is ε_{cc} . The initial values are the unconfined peak concrete strength (f'_{co}), and the Poisson's ratio (v_{co}) usually ranging between 0.1 and 0.3.

The bigger is the hole, the higher is the deformability of the element and the circumferential stresses compared to the radial component: in the case of solid section the dilation of concrete is restrained by the FRP wraps and this interaction yields a strength improvement, while in the case of thin walls, the larger deformability does not allow to gain such strength improvements, even though a significant ductility development is achieved.

3.3 Adopted confined concrete constitutive laws

To simulate the effect of the FRP confinement the two abovementioned approach has been adopted. *Spoelstra & Monti (1999)* model and the model recommended by the *CNR DT200 (2004)* Italian Instructions have been adapted in the first approach₍₁₎.

Compared to these two confinement models₍₁₎, adapted to simulate the behavior of hollow square columns by considering the effect of confinement of single walls, the proposed confinement model, denoted with subscript ₍₂₎, gives a confined concrete strength, corresponding to the peak unconfined strain (0.2%), in-between the previous ones. The main difference is in the subsequent branch, where an almost constant plastic behavior for the hollow section is predicted instead of a hardening branch, common in highly confined solid concrete sections (Fig. 5).

4 THEORETICAL-EXPERIMENTAL COMPARISON

4.1 Global behavior

Only the adapted *Spoelstra & Monti (1999)* model₍₁₎ in the following will be considered, because this is an evolution of the *Mander et al. (1988)* model for confined concrete, such as the proposed model₍₂₎ is. *Mander et al. (1988)* model has been considered for unconfined concrete coupled with size effect theory after *Hillerborg (1989)* for the concrete post peak softening.

The proposed confinement model predicts quite well the behavior of hollow section confinement, in particular the strength increment and the remarkable ductility enhancement.

Experimental and theoretical ultimate axial load P and ultimate flexural capacity M of un-strengthened and strengthened columns corresponding to the eccentricity e related to each specimen are reported in table 3. The proposed model predictions usually underestimate the experimental outcomes with a scatter in the order of about ten percent.

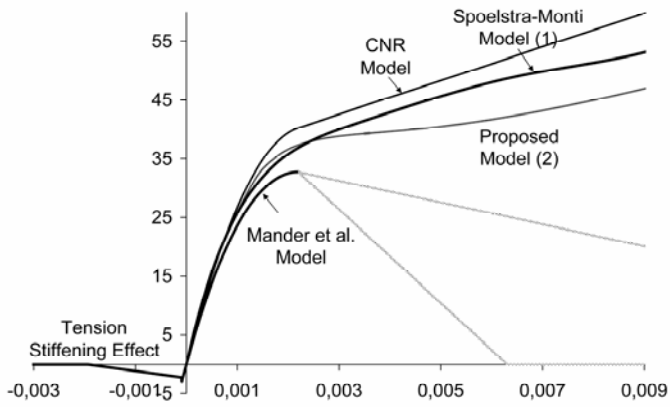


Figure 5. Theoretical confined concrete constitutive laws (hollow section).

The effect of confinement, on the contrary, is reliably evaluated when theoretical predictions for unstrengthened and corresponding strengthened elements are considered (the same strength increments and curvature ductility increments as experimentally found in performed tests are predicted).

Table 3. Experimental-Theoretical failure loads comparison

Specimen Code	e [mm]	P [kN]	M [kNm]	M Error exper. vs. theor.
U1	52	2264	117.73	+11.09%
		2038	106.00	
U2	200	939	187.73	-0.32%
		942	188.39	
U3	300	612	183.64	+7.18%
		571	171.36	
S1	80	2138	171.03	+9.87% ₍₁₎
		1946	155.72	+8.36% ₍₂₎
		1973	157.81	
S2	200	1082	216.48	+3.54% ₍₁₎
		1045	208.91	+2.66% ₍₂₎
		1054	210.82	
S3	300	697	209.20	+12.06% ₍₁₎
		622	186.52	+13.15% ₍₂₎
		616	184.82	

4.2 Deformability

As already mentioned, confinement does not change actual failure mode (steel reinforcement compressive bars buckling and concrete cover spalling), but it is able to delay bars buckling and to let compressive concrete strains attain higher values, thus resulting in higher load carrying capacity of the column and ductility. The increase in confined concrete strength turned into load carrying capacity increase mainly in the columns loaded with small eccentricity (it is clear that close to pure bending load the effect of concrete strength enhancement - i.e. due to confinement - is insignificant because failure swaps to tension side). At lower levels of axial load also the brittle effect of reinforcement buckling is less noticeable. However in small loading eccentricity

cases, concrete ductility and stresses are increased significantly thus resulting also in strength and ductility improvements.

The experimental theoretical comparison of concrete strains at peak (ϵ_{max}) and at 80% of peak load ($\epsilon_{80\%max}$) on the softening branch is shown in table 4. The model is able to predict quite well this deformability aspect and a clear trend is found: concrete strains both at peak and on the softening branch at 80% of peak load increases when eccentricity increases. This fact is due to the brittle failure mechanisms prevailing when higher level of axial load is applied (this is not confirmed by S2 experimental test and this can be due to the formation of the plastic hinge outside the instrumented portion of the tested element: lower ductility was found experimentally in the instrumented section compared to S1). For example, in S3 column the concrete reached strains up to 15‰.

The concrete strains at 80% of peak load are not available in the case of analyses carried out considering adapted *Spoelstra & Monti (1999)* confined concrete model₍₁₎ because the post peak predicted behavior was characterized by an inaccurate hardening branch and it was not possible to evaluate the behavior of the hollow section on the softening branch at 80% of peak load.

Table 4. Experimental-Theoretical deformability comparison

Specimen Code	ϵ_{max} [‰]	$\epsilon_{80\%max}$ [‰]	μ_{χ} [-]	μ_{χ} Error exper. vs. theor.
U1	2.2	2.2	1.00	+0.00%
	2.2	2.4	1.00	
U2	2.6	2.6	1.00	+0.00%
	2.4	2.8	1.00	
U3	2.8	2.8	1.54	-21.13%
	2.4	3.0	1.95	
S1	3.1	9.5	4.24	-4.98% ₍₂₎
	3.0	10.0	4.46	
S2	2.8	5.9	3.02	-40.08% ₍₂₎
	3.2	13.0	5.04	
S3	3.5	15.4	8.27	-7.59% ₍₂₎
	3.4	15.0	8.95	

A comparison between theoretical and experimental strain development is shown in figure 6. The numerical model (dashed line according to the two theoretical approaches) can predict reasonably well the experimental strain evolution (solid line).

One of the major improvements in member behavior due to FRP wrapping is highlighted considering that in unstrengthened columns, when steel reinforcement reaches in compression the buckling stress, as it pushes outward surrounding concrete, the concrete cover spalls out. In the case of members wrapped with FRP, the steel bars, when buckling occurs, push internal concrete unrestrained cover in the inward direction (in the hollow part) only. In the numerical analysis the global response deteriorate

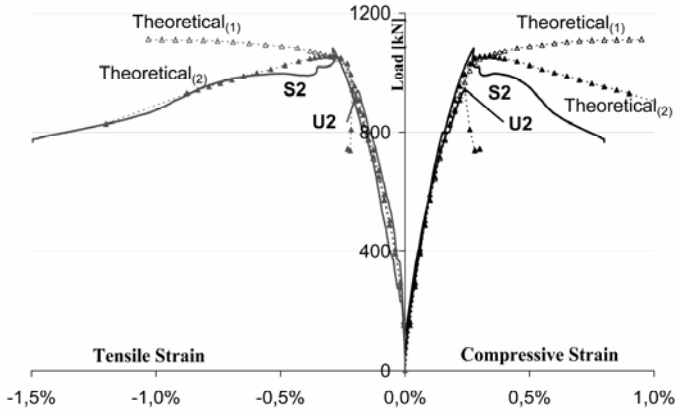


Figure 6. Strain development: U2-S2 Theoretical-experimental comparison.

when concrete cover starts spalling and compressed steel reinforcement bars buckles. The branch after peak is better predicted adopting stress-strain curves for confined concrete with descending branch after peak (i.e. proposed model (2) prediction).

In the case of flexural elements, the ductility can be evaluated at section level by considering the moment-curvature diagrams (Fig. 7) other than comparing concrete strains at material level.

Rotations in potential plastic hinges are the most common and desirable source of inelastic structural deformations. For elements failing in flexure the curvature ductility μ_χ gives a measure of the ductility of the cross section that gives information about the shape of the descending branch in moment-curvature relationships. The curvature ductility can be defined as the ratio of the curvature on the softening branch at 80% of ultimate load, $\chi_{80\%max}$, and the yielding curvature, χ_y (corresponding to the yielding flexural moment M_y). It is pointed out that the curvature ductility is one for the unstrengthened columns U1 and U2: this is due to the sudden bearing capacity drop that does not allow any curvature increment after-peak (i.e., yielding of steel bars was not attained).

In the strengthened S series, it is clearly pointed out the benefit of confinement. Confinement allows the development of larger curvatures after peak load and curvature ductility is larger than three for all the strengthened columns (Tab. 4).

4.3 Specific Energy

For specimens U3 and S3 it can be observed that the increase of μ_χ from 1.54 to 8.27 corresponds also to a significant gain in terms of area under the curve that is proportional to the specific energy.

The increment of ductility supplied by confinement can be also appreciated comparing the values of the specific energies obtained (Tab. 5) and re-

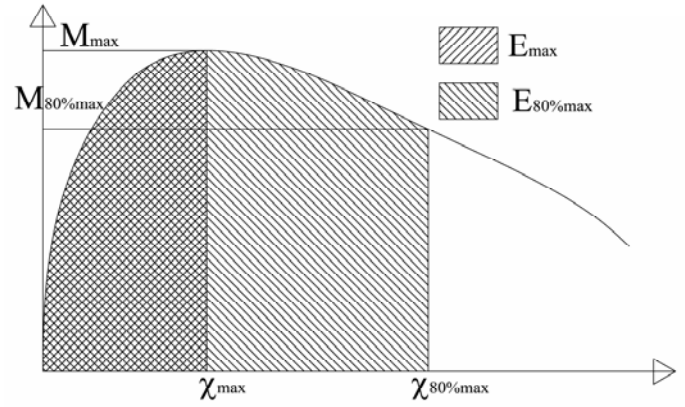


Figure 7. Illustrative Moment vs. Curvature diagram and Specific Energy evaluation

markable increases of dissipating capabilities for strengthened columns are found. Energy values are computed as the area under the Moment vs. curvature diagram at any given χ (refer to illustrative Figure 7).

Table 5 shows the comparative study of the theoretical and experimental specific energy, E . The experimental results were noted to be close to the theoretical predictions with a higher scatter in the case of S2 specimen (for the cited effect of plastic hinge formed far from the instrumented portion of the column).

Table 5. Experimental-Theoretical specific energy comparison

Specimen Code	E_{max} [N]	$E_{80\%max}$ [N]	$\frac{E_{80\%max}}{E_{max}}$	E ratio Error exper. vs. theor.	
U1	exper.	398	398	1.00	+0.00%
	theor.	393	393	1.00	
U2	exper.	1462	1462	1.00	+0.00%
	theor.	1657	1657	1.00	
U3	exper.	3375	3375	1.00	+0.00%
	theor.	2824	2824	1.00	
S1	exper.	1183	4797	4.05	n.a. ⁽¹⁾ -11.38% ₍₂₎
	theor ₍₁₎	854	n.a.	n.a.	
	theor ₍₂₎	988	4512	4.57	
S2	exper.	2134	7907	3.71	n.a. ⁽¹⁾ -20.73% ₍₂₎
	theor ₍₁₎	2416	n.a.	n.a.	
	theor ₍₂₎	2788	13,042	4.68	
S3	exper.	5615	23,113	4.12	n.a. ⁽¹⁾ -15.40% ₍₂₎
	theor ₍₁₎	4473	n.a.	n.a.	
	theor ₍₂₎	3733	18,176	4.87	

The maximum values of ductility, μ_χ , and specific energy ratio are provided by the column S3. For instance, (Tab. 4-5) when predicted μ_χ is 8.95 (while experimental outcome is 8.27), for the same eccentricity the dissipated specific energy, $E_{80\%max}$, of S3 specimen computed on the softening branch at 80% of ultimate load is more than 7 times the dissipated specific energy at peak, E_{max} , of the brittle U3 specimen. Specific energy increment $E_{80\%max}/E_{max}$, (Tab. 5) in S series' columns, is about 4 emphasizing

the meaningful increase of ductility and energy dissipation of the confined structural elements.

4.4 Remarks on the selection of the confined concrete constitutive law

Softening in material constitutive law leads to softening behavior in the section and in the structural element. In a section without rebar buckling, only concrete has a softening behavior: thus moment-curvature relationship softens only in presence of high axial compression force. If steel also has a softening behavior due to buckling, the response of the section becomes softening for any value of axial force. The Mander et al. model compared with the adapted Spoelstra & Monti⁽¹⁾ and the proposed⁽²⁾ model have been considered in the previous comparisons. Both models are calibrated for solid circular cross sections and have been extended and adapted to the case of those square hollow.

The Spoelstra & Monti model has been adapted also to account for the confinement of a hollow section divided into four connecting walls. The effect of confinement is overestimated in the post-peak branch where in reality the presence of the internal void reduces the efficiency of the confinement exerted by the FRP wraps. This model has been adapted and can be successfully used to predict essentially the strength of the column (corresponding roughly to the occurrence of buckling of the compressed steel reinforcement bars). Since it presents an unrealistic hardening behavior after peak, as a consequence it is not able to simulate reasonably the post peak behavior of hollow core sections.

The proposed confinement model predicts quite well the behavior of hollow section confinement. In contrast to the case of solid section, in the case of thin walls, the larger deformability of the concrete element does not allow to gain significant strength improvements, even though a significant ductility development is achieved.

5 CONCLUSIONS

The proposed confinement model, coupled with the proposed computation algorithm is able to predict the fundamentals of the behavior of hollow members confined with FRP both in terms of strength and ductility giving a clear picture of the mechanisms affecting the response of this kind of element. The same strength increments and curvature ductility increments as experimentally found in performed tests are predicted.

The model is able to trace the occurrence of the brittle mechanisms, namely concrete cover spalling and reinforcement buckling, the evolution of stresses and strains in the confinement wraps and concrete allowing to evaluate at each load step the multiaxial

state of stress and the potential failure of the external reinforcement. The main output of the proposed model is also the assessment of the member deformability in terms of both curvature ductility and specific energy. Theoretical results, in satisfactory agreement with authors' experimental data, show that FRP jacketing can enhance the ultimate load and significantly the ductility also in the case of hollow concrete cross sections and under combined compression and flexure loads.

6 ACKNOWLEDGMENTS

The analysis of test results was developed within the activities of Rete dei Laboratori Universitari di Ingegneria Sismica – ReLUIS for the research program funded by the Dipartimento di Protezione Civile – Progetto Esecutivo 2005-2008. The FRP strengthening of the columns was supported by MAPEI Spa., Milan, Italy.

REFERENCES

- Braga, F., Gigliotti G. & Laterza, M. 2006. Analytical Stress-Strain Relationship for Concrete Confined by Steel Stirrups and/or FRP Jackets. *Journal of Structural Engineering*, 132(9):1402-1416.
- CNR-DT 200. 2004. *Guide for the Design and Construction of Externally Bonded FRP Systems for Strengthening Existing Structures*, Published by National Research Council, Roma, Italy.
- Cosenza E. & Prota A. 2006. Experimental behavior and numerical modeling of smooth steel bars under compression. *Journal of Earthquake Engineering*, 10(3):313-329.
- Fam, Amir Z. & Rizkalla, Sami H. 2001. Confinement Model for Axially Loaded Concrete Confined by FRP Tubes, *ACI Structural Journal*, 98(4):251-461.
- Hillerborg A. 1989. The compression stress-strain curve for design of reinforced concrete beams. *Fracture Mechanics: Application to Concrete*, ACI SP-118:281-294.
- Li J. & Hadi M.N.S. 2003. Behavior of externally confined high-strength concrete columns under eccentric loading. *Journal of Composite Structures*; 62:145-153.
- Lignola G.P. 2006. *RC hollow members confined with FRP: Experimental behavior and numerical modeling*. Ph.D. Thesis, University of Naples, Italy.
- Lignola G.P., Prota A., Manfredi G. & Cosenza E. 2007a. Experimental performance of RC hollow columns confined with CFRP. *ASCE Journal of Composites for Construction*, 11(1):42-49
- Lignola G.P., Prota A., Manfredi G. & Cosenza E. 2007b. Deformability of RC hollow columns confined with CFRP. *ACI Structural Journal*, in press.
- Mander J.B., Priestley M.J.N. & Park R. 1988. Theoretical stress-strain model for confined concrete. *ASCE Journal of Structural Engineering*, 114(8):1804-1826.
- Prota A., Manfredi G. & Cosenza E. 2006. Ultimate behavior of axially loaded RC wall-like columns confined with GFRP. *Composites: pt. B, ELSEVIER*, vol. 37:670-678.
- Spoelstra MR & Monti G. 1999. FRP-confined concrete model. *ASCE Journal of Composites for Construction*, 3(3):143-150.